

Laser with continuous frequency tuning in the visible range, based on stimulated Raman scattering by polaritons

A M Bel'skii, I M Gulis, K A Saechnikov

Abstract. Continuous frequency tuning was demonstrated experimentally for a YAG:Nd³⁺ laser system with stimulated Raman scattering by polaritons and nonlinear frequency summation in LiIO₃ crystals. A theoretical description was developed for the tuning characteristics on the basis of a calculation of the dependence of the frequency of a polariton mode on its wave vector.

A solid-state YAG:Nd³⁺ laser with continuous pumping and passive mode locking has been described earlier [1]. In this laser an LiIO₃ crystal located inside the resonator cavity simultaneously performs the functions of a Raman-active medium and of a nonlinear frequency converter: in this crystal the stimulated Raman scattering (STRS) components are summed with the fundamental-frequency radiation, so that for certain orientations of the crystal the output radiation is in the visible range. The emission at eight wavelengths in the range 509–612 nm is reported in Ref. [1]. In the laser with two crystals (an intracavity crystal acting as a Raman-active medium and an extracavity crystal performing the function of a nonlinear frequency converter) the emission involves participation of a polariton mode. The dependence of the frequency of polariton oscillations on the wave vector [2] provides an opportunity for continuous tuning of the output radiation frequency by rotation of the intracavity crystal. The present paper reports an experimental and theoretical investigation of such continuous frequency tuning.

Our apparatus was similar to that described in Ref. [1]. In some experiments an acousto-optic modulator was included in the resonator cavity; the most stable emission was obtained when this modulator operated at 1 kHz.

For example, when the intracavity crystal was oriented so that the electric vector of the fundamental-frequency wave was in the principal plane of the crystal (extraordinary wave), collinear STRS on the vibrational mode $\nu_p \sim 650 \text{ cm}^{-1}$ occurred (in Ref. [1] it was attributed to a polariton oscillation of a mixed $A + E_1$ symmetry). The intracavity crystal acted as the Raman-active medium in which the following multistage stimulated scattering process took place:

$$\nu_0 - m\nu_p \rightarrow \nu_0 - (m + 1)\nu_p, \quad m = 0, 1, 2. \quad (1)$$

All the waves propagated in the crystal as extraordinary (e) waves. The following process of nonlinear phase-matched

frequency summation took place in the extracavity crystal:

$$\nu_0 + [\nu_0 - (m + 1)\nu_p] \rightarrow 2\nu_0 - (m + 1)\nu_p, \quad m = 0, 1, 2. \quad (2)$$

For each of the three investigated waves the extracavity crystal was tuned to ensure phase matching for the relevant summation process. Rotation of the intracavity crystal resulted in a smooth variation of all three wavelengths formed as a result of the summation process (2). The quantity $\Delta\alpha$ in Fig. 1 represents the angle of rotation of the intracavity crystal in its principal plane ($\Delta\alpha = 0$ corresponds to coincidence of the resonator axis with the phase-matching direction for second-harmonic generation). The results presented in Fig. 1 can be interpreted on the assumption that rotation of the crystal alters the polariton mode frequency ν_p because of a change in its wave vector.

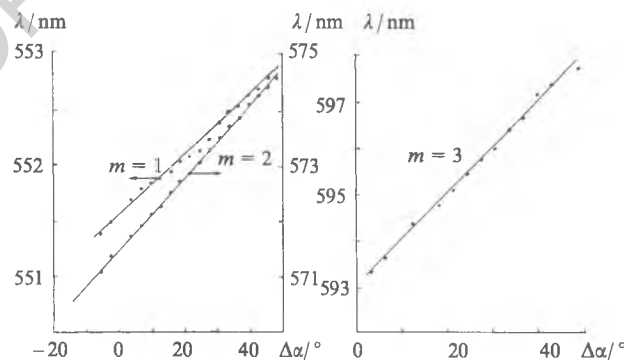


Figure 1. Experimental dependences of the emission wavelengths of a solid-state YAG:Nd³⁺ laser on the angle of rotation of a nonlinear LiIO₃ crystal placed inside the laser resonator. Phase matching was performed by a second (extracavity) LiIO₃ crystal. The parameter m determines the frequency of the scattered wave.

The anisotropy of the crystal field and the presence of long-range fields induced in a crystal in the case of dipole-active lattice vibrations give rise to the following dependence of the frequency of polariton oscillations on the wave vector \mathbf{K} (in the specific case of a uniaxial crystal and oscillations of the mixed $A + E_1$ symmetry) [3]:

$$K_p^2 = \frac{4\pi^2 \nu_p^2}{\sin^2 \theta \left(\frac{\sigma_A}{\epsilon_e^\infty} \right) + \cos^2 \theta \left(\frac{\sigma_{E1}}{\epsilon_o^\infty} \right)}, \quad (3)$$

$$\sigma_A = \prod_{i=1}^{N_A} \frac{(\nu_{Ai}^{TO})^2 - \nu_p^2}{(\nu_{Ai}^{LO})^2 - \nu_p^2}, \quad \sigma_{E1} = \prod_{i=1}^{N_{E1}} \frac{(\nu_{E1i}^{TO})^2 - \nu_p^2}{(\nu_{E1i}^{LO})^2 - \nu_p^2},$$

where $\nu_{A;E1}^{TO;LO}$ are the fundamental frequencies of the transverse and longitudinal oscillations of the A and E_1

A M Bel'skii, I M Gulis, K A Saechnikov State University, Minsk, Belarus'

Received 24 June 1993

Kvantovaya Elektronika 21 (4) 371–372 (1994)

Translated by A Tybulewicz

symmetry, respectively; N_A and N_{E1} are the numbers of different fundamental frequencies of oscillations of the A and E_1 symmetry; ε_o^∞ , ε_e^∞ are the high-frequency permittivities for the ordinary and extraordinary waves; θ is the angle between the wave vector of the polariton oscillations and the optic axis of a crystal.

The dispersion curves $\nu_p(\mathbf{K})$ calculated on the basis of the system of equations (3) are shown in Fig. 2 (curves 1–7). These curves are plotted for the following parameters: $\varepsilon_o^\infty = 3.61$, $\varepsilon_e^\infty = 3.06$; $\nu_A^{TO} = 148, 238, 354$, and 795 cm^{-1} ; $\nu_A^{LO} = 149, 239, 490$, and 812 cm^{-1} ; $\nu_{E1}^{TO} = 180, 330, 360$, and 769 cm^{-1} ; $\nu_{E1}^{LO} = 181, 340, 460$, and 845 cm^{-1} . We can see from Fig. 2 that the frequency of the polariton oscillations depends on the wave vector \mathbf{K} ; on the other hand, the modulus of \mathbf{K} is determined by the law of conservation of momentum in the STRS process; for the scattering process described by Eqn (1) this law can be written in the form

$$K_p = K_i - K_s = \frac{2\pi}{c} (\nu_i n_i - \nu_s n_s), \quad (4)$$

where the indices i and s refer to the incident and the scattered wave, respectively. Since in the scattering case described by Eqn (1) both waves are extraordinary, Eqn (4) can be written in the form

$$K_p = \frac{2\pi}{c} \{ (\nu_0 - m\nu_p) n_e(\theta; \nu_0 - m\nu_p) - [\nu_0 - (m+1)\nu_p] n_e(\theta; \nu_0 - (m+1)\nu_p) \}, \quad (5)$$

which gives the implicit dependence of $\nu_p(K_p, \theta)$. Simultaneous solution of Eqns (3) and (5) gives the dependence of the frequency ν_p of the polariton oscillations on the angle θ of propagation of the scattered wave.

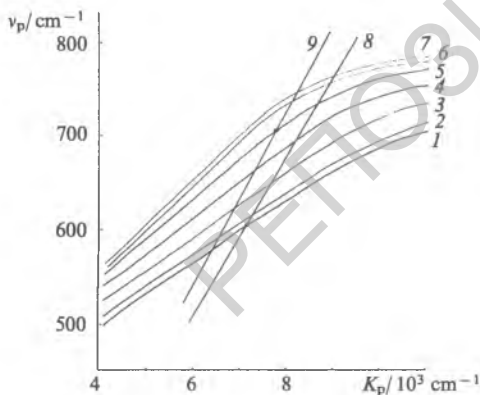


Figure 2. Dispersion curves of an oblique polariton in the vicinity of the frequency $\nu_p \sim 630 \text{ cm}^{-1}$ (1–7) and dependences $K_p(\nu_p)$ for $m = 8$ (8, 9). The angle between the optic axis and the direction of polariton propagation is $\theta = 0^\circ$ (1, 8), 15° (2), 30° (3), 45° (4), 60° (5, 9), 75° (6), and 90° (7).

Since the wavelength of the Stokes component does not differ greatly from the wavelength of the scattered radiation, Eqn (5) can be written in a simpler form by expanding the refractive index as a Taylor series in λ :

$$K_p = 2\pi \left[n_e(\theta; \lambda_0) - \lambda_0 \frac{\partial n_e}{\partial \lambda} \Big|_{\lambda_0} - (m + \frac{1}{2}) \lambda_0^3 \frac{\partial^2 n_e}{\partial \lambda^2} \Big|_{\lambda_0} \bar{\nu}_p \right] \bar{\nu}_p, \quad (6)$$

where $\bar{\nu}_p \equiv \nu_p/c$.

The dependences $K_p(\nu_p)$ obtained from Eqn (6) for two values of θ when $m = 0$ are plotted in Fig. 2. The points of intersection of the $K_p(\nu_p)$ curves obtained from Eqn (6) with the corresponding dispersion curves (for the same angles θ) determine the frequencies of the polariton oscillations that appear as a result of collinear scattering along the given direction θ . It is worth noting the weak dependence of the wave number K_p in Eqn (6) on the integer m : this dependence is due to the dispersion of the refractive indices and it has the effect that for the same angle θ the polariton oscillation frequency (and, consequently, the shift of the Stokes component) is different for the three scattering processes described by Eqn (1). In other words, the dispersion makes the Stokes shift dependent on the frequency of the scattered wave.

The tuning curves, i.e. the dependences $\nu_p(\theta)$, plotted in Fig. 1 are obtained by simultaneous solution of Eqns (3) and (6). The dispersion dependences of the refractive indices are found from the Sellmeier expressions [4]. The angle $\Delta\alpha$ is converted to the angle θ in accordance with

$$\sin^2 \Delta\alpha = \frac{\varepsilon_o(\lambda_0) \varepsilon_e(\lambda_0) \sin^2(\theta - \theta_{pm})}{\varepsilon_o(\lambda_0) \sin^2 \theta + \varepsilon_e(\lambda_0) \cos^2 \theta},$$

where θ_{pm} is the phase-matching angle for second-harmonic generation. The points in Fig. 3 represent the experimental values deduced from the tuning curves (see Fig. 1).

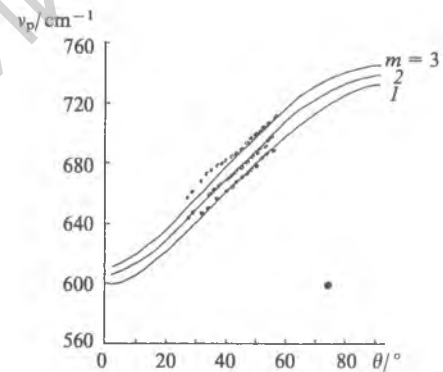


Figure 3. Dependences of the frequency of a polariton on the direction of its propagation in the case of collinear STRS. The points on the curves are the experimental values. The parameter m determines the frequency of the scattered wave.

There is thus a good agreement between the experimental and theoretical dependences. The feasibility of continuous tuning of the emission frequency makes the proposed source promising for practical applications. The range of the STRS-active media in which tuning is possible because of the scattering by polaritons can be extended and, consequently, a greater range of working spectral intervals can be covered.

This work was financed by the 'Lazer' Republican Programme of Belarus'.

References

1. Bel'skiĭ A M, Gulis I M, Mikhailov V P, et al. *Kvantovaya Elektron. (Moscow)* 19 769 (1992) [*Sov. J. Quantum Electron.* 22 710 (1992)]
2. Merten L *Phys. Status Solidi* 30 449 (1968)
3. Otaguro W S, Wiener-Avneer E, Porto S P S, et al. *Phys. Rev. B* 6 3100 (1972)
4. Prokhorov A M (Ed.) *Spravochnik po Lazeram* (Handbook on Lasers) (Moscow: Sovet-skoe Radio, 1978)